Contact Resistance Between REBCO Coated Conductors in the Presence of a V_2O_3 Inter-Layer

Bonura, Marco; Bovone, Gianmarco; Cayado Llosa, Pablo; Senatore, Carmine

How to cite

BONURA, Marco et al. Contact Resistance Between REBCO Coated Conductors in the Presence of a V_2O_3 Inter-Layer. In: IEEE transactions on applied superconductivity, 2023, vol. 33, n° 5. doi: 10.1109/TASC.2023.3251291

This publication URL: https://archive-ouverte.unige.ch/unige:168586
Publication DOI: 10.1109/TASC.2023.3251291

Contact Resistance between REBCO Coated Conductors in the presence of a V_2O_3 inter-layer.

M. Bonura, G. Bovone, P. Cayado, and C. Senatore

***Abstract*—We report a study of the contact resistance between commercial Cu-stabilized REBCO tapes coated with V_2O_3, which is a functional material that passes through a metal-to-insulator transition at cryogenic temperatures. We prove that a simple dip coating technique, potentially scalable to coat long-length conductors, allows the deposition of ~10-μm-thick V_2O_3 layers. We find that the contact resistance between the REBCO tapes is mainly determined by the properties of the V_2O_3 layer and that it varies by more than 8 orders of magnitude from 10 K to room temperature. Based on our experimental results and on previous studies [1], we deduce that an effective quench propagation may take place in REBCO pancake coils when the hot spot temperature is in the range 135 K – 175 K, depending on the V_2O_3 layer thickness. Because of the metal-to-insulator transition of the V_2O_3, the contact resistance rapidly increases at lower temperatures, assuming values comparable with those of insulated coils. In a general perspective, the results of this research can help magnet designers to assess the role of metal-to-insulator-transition materials for future REBCO-based magnets.**

***Index Terms*— Coated conductors, contact resistance, metal to insulator transition, V_2O_3, REBCO.**

I. Introduction

Protection against quenches has been one of the major issues associated with the use of $REBa_2Cu_3O_{7-x}$ coated conductors (REBCO CCs, RE= rare earth) in magnet technology, as the propagation velocity of a normal spot in high-temperature superconductors is much slower than in low-temperature ones [2, 3]. The no-insulation (NI) winding technique proved to be a viable solution to achieve self-protection against quenches in REBCO pancake coils [4, 5]. This technique may represent an important step forward in the widespread use of REBCO CCs for high field magnets, which would not need complex protection systems for the HTS coil [6]. The NI technique has intrinsic demerits, too, as nonlinearities into the field-current characteristic and a delay in reaching the desired magnetic field [7, 8]. The use of a proportional-and-integral feedback control for the magnet power supply was shown to mitigate these drawbacks, although it does not permit to reach the field stability required for NRM or MRI systems [7, 9]. Quench propagation in NI pancake coils is mainly an inductive process [1, 10]. When a hot spot develops in a pancake, the current can flow radially due to the absence of insulation. This generates large transient azimuthal currents (above the critical current, I_c) in the other pancakes, leading to a fast propagation of the quench in the whole magnet [1]. However, the transient radial currents generated during a quench give rise to unbalanced mechanical loads that may lead to irreversible mechanical damages [7, 11, 12].

The contact electrical resistance between the coil layers, R_s, is the key parameter to model the electromagnetic response of REBCO magnets and, thus, to evaluate the mechanical loads during a quench, too [1, 11]. In the case of no insulation between the CCs, R_s typically spans in the range $1 - 10^2$ μΩ·cm^2, and is much influenced by the oxide layer that spontaneously forms on the Cu-stabilizer surface when exposed to air [13, 14, 15]. An important work from Markiewicz *et al.* proved that an effective quench propagation can take place in REBCO pancake coils also in the case of a higher R_s, in the range $10^3 - 10^5$ μΩ·cm^2 [1]. The size of the coil plays a role in determining the maximum R_s that allows an effective quench propagation: the bigger the coil, the higher the R_s. This is a consequence of the inductive nature of the quench propagation in this family of magnets [1, 10]. Variants of the NI technique have thus been proposed in an attempt to tailor the R_s and achieve self-protection against quenches limiting the drawbacks due to the absence of electrical insulation. The metal co-winding and the partial insulation techniques are examples of these variants [11, 16, 17]. Recently, Lecrevisse *et al.* reported about a REBCO coil co-wound with stainless steel [11]. This coil was successfully protected by a conventional protection system based on voltage detection, thanks to a relatively high R_s, in the range $1 - 3 \times 10^5$ μΩ·cm^2 [11]. With the same aim to reach R_s values that are in-between those of NI and insulated coils, the manufacturer SuNAM proposed the "metallic cladding" approach, where a μm-thick stainless-steel layer is coated over the REBCO CC [18].

In the NI technique and its variants, the variation of R_s with the temperature is mainly determined by the properties of the material that contributes the most to the overall surface resistance, i.e., the one with the largest product $\rho \cdot t$, where ρ is the electrical resistivity of the material and t the thickness of the relative layer. If one excludes the contribution to the measured resistance due to the superconducting transition of the REBCO

M. Bonura is with the Department of Quantum Matter Physics of the University of Geneva, Switzerland (e-mail: Marco.Bonura@unige.ch). G. Bovone is with the Department of Quantum Matter Physics of the University of Geneva, Switzerland (e-mail: Gianmarco.Bovone@unige.ch). P. Cayado is with the Department of Quantum Matter Physics of the University of Geneva, Switzerland (e-mail: Pablo.Cayado@unige.ch). C. Senatore is with the Department of Quantum Matter Physics of the University of Geneva, Switzerland (e-mail: Carmine.Senatore@unige.ch).

Color versions of one or more of the figures in this paper are available online at http://ieeexplore.ieee.org.

layer at T_c [14], the variation of R_s from room temperature to 4.2 K is expected to be $\lesssim 1$ order of magnitude (2 orders of magnitude would mean than the material with the highest $\rho \cdot t$ has a residual resistivity ratio of ~ 100). The use of materials that undergo a metal-to-insulator transition (MIT) upon lowering the temperature was proposed to tune R_s with the temperature on a much wider extent [19, 20, 21]. The idea behind is to take advantage of a very high R_s at the magnet working temperature, as in insulated coils. However, if a hot spot develops in the winding, the raise of temperature may be locally reduced by several orders of magnitude R_s. This would allow the flow of the current in the radial direction in correspondence of the hot-spot, similarly to what occurs in NI coils, and possibly enable self-protection against quenches. In its single-crystal form, V_2O_3 shows a sharp MIT transition at about 150 K with a variation in the electrical resistivity by 6 – 7 orders of magnitudes [22, 23]. The width and amplitude of the transition observed in $\rho(T)$ depend on different factors, including the structural properties and the homogeneity of the V_2O_3 phase [23, 24, 25, 26]. The low temperature at which the metal-to-insulator transition occurs, and the fact that V_2O_3 is readily available on the market in the form of powders, make this material a promising candidate for practical use in magnets. To the best of our knowledge, no experimental studies have been reported about the R_s in REBCO CCs coated with a MIT layer. We consider this investigation fundamental to assess the advantages associated with the possible use of this class of materials in HTS-based magnets. This paper reports a study of the R_s between REBCO CCs coated with V_2O_3. We describe the technique we used to deposit the MIT layer on commercial Cu-stabilized CCs. Furthermore, we identify the range of temperatures at which it is expected to have radial currents intense enough to lead to an effective quench propagation in REBCO pancake coils.

II. Experimental Technique

We coated commercial Cu-stabilized REBCO CCs (manufacturer: Fujikura, product code: FESC-SCH04, substrate thickness: 50 μm, Cu stabilizer thickness: 2 × 40 μm) with a V_2O_3 layer by dip-coating. We opted for this technique because of its simplicity and potential scalability (e.g., via spray-coating) for long-length conductors. We purchased V_2O_3 powders with a nominal purity of 99.9 %. The as-bought powders had an inhomogeneous granulometry in the range 10 – 100 μm, as evaluated by scanning-electron microscopy. We ball milled the as-purchased powders for 72 h at low speed to reduce their size. The granulometry after the milling process was in the range of ~ 1 μm. We used the milled powders to prepare colloidal solutions in ethanol. After a few tests about the viscosity of the colloidal solution and the wettability of the CC surface, we decided to fix the concentration of the MIT powders in the solution to 30 wt.%. Furthermore, we investigated the use of a polymer to enhance the viscosity of the solution. For this purpose, we prepared colloidal solutions of V_2O_3 powders (30 wt.%) and Polyvinyl butyral (PVB, 1 wt.%) in ethanol.

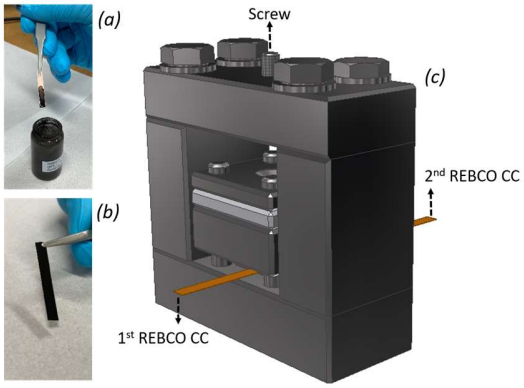

Fig. 1. Moments of the procedure adopted to coat commercial REBCO CCs with a V_2O_3 layer (a), (b). Device used to measure the contact resistance as a function of the pressure applied on the CCs' contact area (c).

Panels (a) and (b) of Fig. 1 show some of the steps of the dip coating procedure. First, we removed the oxide layer from the Cu stabilizer by chemical etching in a 50 vol.% CH_3COOH - 50 vol.% H_2O solution, as described in [13]. The etching procedure typically lasted a few hours. The CC was successively rinsed in ethanol, dried, and manually dipped into the colloidal solution for ~ 1 s. The colloidal solution was stirred several minutes before dipping. For each CC, the dipping process was repeated 2 to 6 times to achieve a full coating of the CC surface, tuning the thicknesses of the MIT layer. After the last dip, the CC was dried in air for ~ 1 hour to let the ethanol evaporate. Subsequently, we prepared sandwiches of CCs coated with the V_2O_3 as schematically shown in Fig. 2 (a). The overlap area is about 16 mm^2. We used the device shown in Fig. 1 (c) to apply pressure in the overlap region of the CCs using a torque wrench. The setup was calibrated by means of pressure-measurement films from Fujifilm, as detailed in [13]. Thermal treatments can enhance the connectivity of the layer prepared by dip coating and improve its adhesion to the Cu stabilizer surface. For this reason, we decided to cure the CCs' sandwiches at 150°C for ~ 30 min applying a pressure of ~ 50 MPa. The temperature of the heat treatment was chosen to avoid the possible degradation of the superconducting properties of the CCs [27]. We did not carry out a dedicated study to evaluate the effect of the curing on R_s.

R_s was assessed by standard 4-point measurements. We used a Keithley 2400 current source-meter, which allows the reading of the actual current circulating in the circuit, and a Keithley 2182A nanovoltmeter to detect the voltage drop. The probing

TABLE I
Samples

Label	V_2O_3 concentration in the colloidal solution	PVB concentration in the colloidal solution	N° of dips per CC	Curing at 150°C for 30 min	MIT layer thickness per each CC
Sample A	30 wt.%	0	6	Yes	45 – 55 μm
Sample B	30 wt.%	0	2	Yes	5 – 10 μm
Sample C	30 wt.%	1 wt.%	4	Yes	30 – 40 μm

Preparation details of the investigated samples. The last column reports the range of thickness of the MIT layer as measured at different positions of the CC using a profilometer.

current was varied in the range 1 μA - 1 mA, depending on the sample and on the investigated temperature range. Fig. 2 (b) shows the electrical circuit reproduced in our experimental configuration. We employed two different experimental probes to study R_s in different temperature ranges. We used the pressure device shown in Fig. 1 (c) to measure R_s from room temperature down to 77 K, and to evaluate the effect of the pressure on R_s at 77 K. We used the probe for electrical transport measurements described in [28] to measure R_s in a wider range of temperatures down to ~ 10 K. This probe was not calibrated to determine the actual pressure acting on the CC sandwich. We measured the thickness of the MIT layers by means of a Tencor™ profilometer from KLA. The images to evaluate the granulometry of the V_2O_3 powders were taken using a Schottky Field Emission Scanning Electron Microscope (model JEOL JSM-760F) by dispersing the MIT powders on a conductive carbon adhesive tape.

III. Experimental Results

For each sample, we first measured R_s from room temperature down to 77 K to verify that the sample preparation procedure was successful. In particular, it is essential that the overlap area between the two CCs is fully coated with the MIT layer. If this is not the case, the MIT transition will have a negligible effect on the measured R_s variation, as the current bypasses the MIT layer through Cu short circuits. We performed several tests, not reported in this work, indicating that the irregularities in the Cu layer thickness, in particular at the edges of the CC (the so-called dog-bone shape), play a role in this regard. In some cases, even if we coated uniformly the CC surface, we observed an electrical short circuit between the CCs after applying the pressure. Visual inspections *post measurement* showed that the stress concentration at the CC edges, due to the dog-bone shape, damaged the MIT layer leaving parts of the Cu stabilizer uncovered. We experienced this kind of problems mainly when preparing sandwiches with only one of the two CCs coated with the MIT layer. For this reason, all the samples investigated in this work were prepared coating with V_2O_3 both the CCs constituting the sandwich. More details about the investigated samples' properties are reported in Table I.

The main figure of Fig. 3 reports the variation of R_s with time as acquired on the Sample A while filling with liquid nitrogen an insulated vessel in which we placed the pressure device shown in Fig. 1 (b). The sample temperature was not acquired during this measurement because the fast cooling did not allow the temperature equilibrium of the sample and, thus, a proper reading of its temperature. R_s increases by ~ 3 orders of magnitude as the temperature decreases from 293 K to 77 K. We applied a pressure of ~ 140 MPa on the sample before starting the cool down. Most of this pressure is released after the cool-down because of the different thermal-contraction coefficients of the materials the device is made of. Therefore, data of the main panel of Fig. 3 cannot be considered as acquired at a constant pressure. Once at 77 K, we measured R_s as a function of the applied pressure. The results of this investigation are reported in the inset of Fig. 3 and provide valuable information about the variation of R_s expected in a coil as a function of the actual stress at the operating conditions. A comparison of data from the main panel and those of the inset allows us to evaluate that the pressure on the sample at the end of the cool-down was $\lesssim$ 20 MPa. R_s decreases with the pressure applied on the CCs' contact area. This result is expected for multiple reasons: i) the connectivity of granular materials normally improves with the packing factor of the powders; ii) the pressure may enhance the adhesion between the powders and the Cu surface; iii) the thickness of the MIT layer may slightly vary with the applied pressure. A decrease of R_s between sandwiches of CCs upon augmenting the applied pressure was previously reported for bare CCs and in case of CCs co-wound with normal metals [13]. In the case of the Sample A, the variation of R_s with the applied pressure was measured twice, without removing the setup from the liquid nitrogen bath. We did not observe any irreversibility in R_s, indicating that the MIT-layer properties of this sample were not modified after applying a pressure up to ~ 300 MPa.

Fig. 4 reports the variation of R_s with the time for the Sample B during a cool-down analogous to the one realized for the Sample A. R_s varies by ~ 3 orders of magnitude from room temperature to 77 K for this sample, too. On the other hand, a comparison with the results of Fig. 3 shows that the R_s is smaller in this sample than in Sample A. We ascribe this difference mainly to the different thickness of the MIT layer in the two samples (see Table I). The inset of Fig. 4 reports the variation of R_s with the pressure as measured at 77 K on this sample.

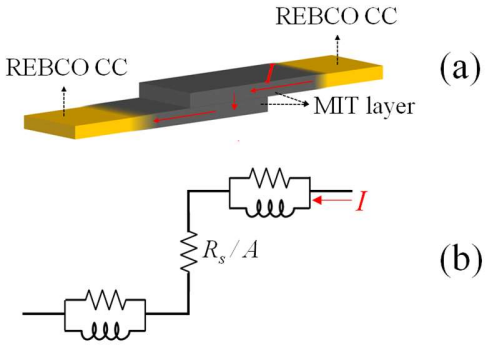

Fig. 2. Schematic drawing showing the layout adopted to measure the contact resistance (R_s) on REBCO CCs coated with a MIT layer (a). Electric circuit associated with the experimental configuration (b).

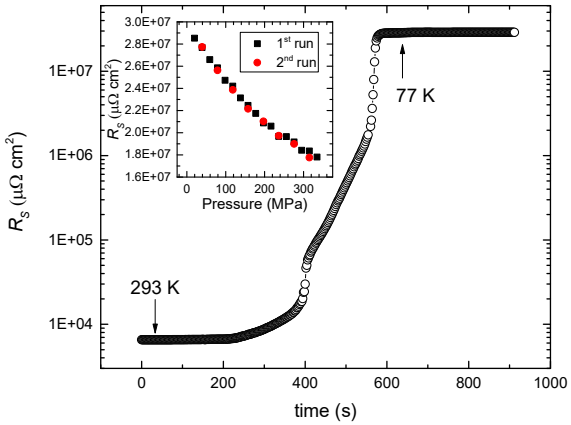

Fig. 3. Main panel: variation of the surface resistance with the time during an uncontrolled cool-down for the sample A. Inset: variation of the contact resistance with the pressure applied on the CC sandwich as measured at 77 K. This measurement was repeated twice to verify the reversibility of the process.

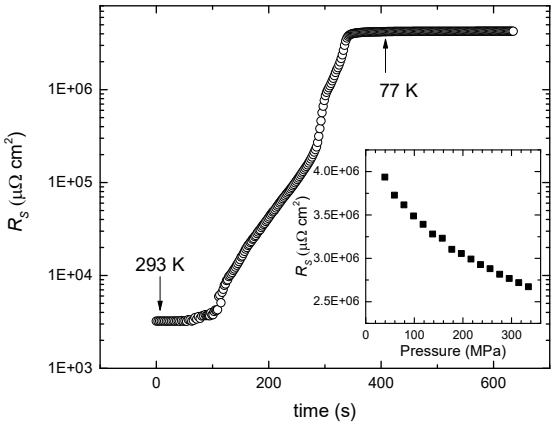

Fig. 4. Variation of the contact resistance with the time during an uncontrolled cool-down for the Sample B. Inset: variation of the surface resistance with the pressure applied on the CC sandwich, as measured at 77 K.

To characterize the variation of R_s in a wider temperature range, we further investigated Sample A by means of a low-noise probe for electrical transport measurements described in [28]. The results of this investigation are reported in Fig. 5. Contrary to the case of the set-up shown in Fig. 1 (c), this probe was not calibrated to evaluate the pressure acting on the CCs' overlap area. However, the obtained R_s vs T dependence can be scaled using the data of Fig. 3 acquired at 77 K as a reference. Indeed, R_s is proportional to the electrical resistivity of the MIT powders, whose temperature dependence is not expected to vary with the pressure in our experiment. In order to allow a comparison in experimental conditions as similar as possible, all the results reported in Fig. 5 are associated with a same pressure of 50 MPa. This value may typically result from the tension applied when winding a solenoid magnet [29]. Considering the layout of the sample holder, we do not expect significant variations of the pressure upon varying the temperature with this measurement probe. In Sample A, the results of Fig. 5 show that R_s varies by ~ 8 orders of magnitude when increasing the temperature from ~ 10 K to ~ 250 K. In particular, R_s becomes smaller than 10^5 μΩ·cm^2 at ~ 175 K. The superconducting transition of the REBCO layer does not lead to any significant variation of R_s. This result agrees with our expectation that the main contribution to R_s comes from the MIT layer. In the case of Sample B, we were not able to measure R_s using this resistivity probe because the sample got damaged during mounting. We remind here that the only difference in the preparation of the samples A and B is the number of times the CCs were dipped into the colloidal solution. Therefore, we do not expect significant variations in the properties of the V_2O_3 layer for the two samples. Since the temperature dependence of R_s is mainly determined by the properties of the V_2O_3 powders, we can reasonably use the $R_s(T)$ dependence measured on Sample A to estimate the one of Sample B. This corresponds to suppose that only the thickness or the connectivity of the MIT layer can differ between the two samples. The dotted line in Fig. 5 was calculated under the above-described assumptions, using the R_s value measured on Sample B at 77 K and 50 MPa (data from Fig. 4) as the reference to scale the $R_s(T)$ curve. For Sample B, R_s is expected to become smaller than 10^5 μΩ·cm^2 at ~ 135 K.

The technique that we adopted to coat commercial CCs easily allowed us to deposit MIT layers whose thickness is in the range of ~ 10 μm. On the other hand, we did not succeed to deposit much thinner MIT layers − in the 1 μm range − achieving a full coverage of the Cu stabilizer surface. This is expected since the granulometry of the powders that we used (~ 1 μm) sets a lower limit to the thickness of the coating layer. Furthermore, we performed the coating procedure manually, therefore without a full control of the various parameters involved in the coating process. The use of viscous colloidal solutions that have a high adherence to the Cu may be a way to obtain more-homogeneous thin-layer coatings. Based on the results of Fig. 5, this might allow a R_s of ~ 10^5 μΩ·cm^2 at temperatures close to the T_c of REBCO. Polymers are often used to enhance the viscosity of colloidal solutions. Hyung-Wook Kim *et al.* prepared a very viscous paste by mixing V_2O_3 powders, a polymer-based binder and a solvent [19, 20, 30]. They used this paste to paint REBCO CCs and prepare pancake coils that were successively tested. This technique did not allow them to control the thickness of the MIT layer, which is determined by the winding tension [21].

To get some clues on the possible use of additives to ease the deposition of MIT layers on CCs by dip coating, we prepared a further sample (Sample C) using a colloidal solution that included a small amount of PVB (1 wt.%). The MIT powders used to prepare this colloidal solution were from the same batch of those used to prepare the samples A and B. PVB is commonly employed in industry, e.g., as an interlayer in the production of laminated safety glasses. Furthermore, it can be used to embed nanometric powders in a polymeric matrix [31]. In our experiment, the use of PVB led to an increase in the viscosity of the colloidal solution. However, we obtained a proper coverage of the whole overlap area between the CCs only after 3 - 4 dips into the colloidal solution. As a consequence, the thickness of the MIT layer of this sample resulted to be in the range ~ 30 – 40 μm, not very different from those of the other samples. The use of a spin coater may allow one to obtain thinner layers in the case of viscous solutions. However, we believe that such an investigation goes beyond the scope of the present paper.

Fig. 5 reports the variation of R_s with the temperature for Sample C, too. The use of PVB leads to R_s values that are ~ 4 orders of magnitude higher than those measured in samples prepared without the polymer. As the thickness of the MIT layers are of the same order of magnitude in all investigated samples (see Table I), and considering that we used a unique batch of MIT powders for all samples, we infer that such a big enhancement of R_s must be due to a reduced electrical connectivity between the MIT powders due to the presence of the polymer. Furthermore, we observed that the R_s measured at room temperature decreased after curing the sample at ~ 150 °C for ~ 30 min under pressure. PVB is expected to melt at an average temperature of ~ 140 °C [32] and a reassessment of the MIT powders is possible when at high temperature. We did not observe any significant variations of R_s after heating the samples prepared without PVB. Because of the high resistance of the MIT layer, we were not able to measure R_s of Sample C at temperatures lower than ~ 125 K, since the current source reached the

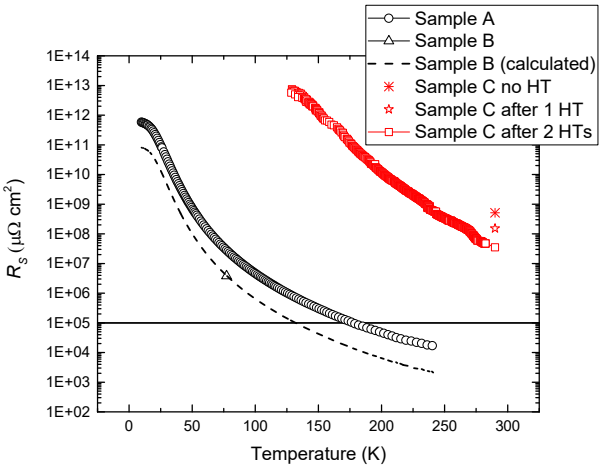

Fig. 5. Variation of the surface resistance with the temperature for the 3 samples investigated in this work. Full points indicate measured values. The dashed line has been calculated under the assumptions specified in the text. All data refer to a same pressure (50 MPa) applied on the CC sandwich.

voltage limit. The fact that nanometric powders were successfully used as fillers in a PVB polymer matrix [31] suggests that a much lower R_s would be possible when using MIT powders with a much finer granulometry than the one used by us.

IV. Discussion

Markiewicz *et al.* reported that an effective quench propagation can take place in REBCO pancake coils when R_s is in the range $10^3 – 10^5$ μΩ·cm² [1]. These figures for R_s are higher than those typically realized in NI coils [13, 15]. For a fixed coil size, the higher the R_s, the smaller the intensity of the transient currents that make the quench propagate. Thus, it exists a maximum value for R_s, at which the effective quench propagation ceases. The fact that an effective quench propagation is achieved for a wide range of R_s may help magnet designers to identify a regime where the quench-induced stresses are limited [1].

The results of Fig. 5 allow us to draw some conclusions about the possible use of V_2O_3 in REBCO coils. In our experiments, the use of PVB leads to a R_s that is too high to ensure the self-protection of the coil in case of quench. However, as already mentioned, we cannot exclude that the use of V_2O_3 powders with a much smaller granulometry than those used in this work can lead to a lower R_s, even in the case of colloidal solutions prepared with PVB. The very high R_s measured at low temperatures for samples A and B points out that a REBCO coil wound using CCs coated with V_2O_3, as per our technical procedure, would behave as an electrical-insulated coil at the magnet operating conditions. On the other hand, the decrease of R_s in correspondence of a hot spot may allow the flow of the current in the radial direction. Assuming for simplicity that $R_s = 10^5$ μΩ·cm² defines the effective quench propagation limit, we expect to have radial currents able to induce an effective quench propagation when the hot spot reaches temperatures in the range 135 K – 175 K, depending of the MIT-layer thickness. A MIT layer whose thickness is in the 1 μm range would allow radial currents at even lower temperatures, comparable with the T_c of the REBCO. It must be specified that, contrary to the case of NI or partially-insulated coils, the use of a MIT inter-layer would allow radial currents only in correspondence of the hot spot. More complete analyses, which consider also the heat diffusion in the MIT layer, should be performed to clearly understand the behavior of this type of magnets in case of quench.

An enhanced stability of REBCO pancake coils co-wound with a V_2O_3 paste was recently reported [19]. Furthermore, a quench-simulation code with an equivalent electric-circuit model was proposed to analyze the electrical and thermal behaviors of these coils [33]. In the simulations, the authors assumed that the metal-to-insulator transition leads to a sudden variation of the electrical resistivity by ~ 7 orders of magnitudes at T~ 150 K. However, they found discrepancies between the experimental and simulation results, which were ascribed to uncertainties in the actual temperature dependence of the electrical properties of the V_2O_3 layer. The results of Fig. 5 (samples A and B) indicate that the variation of R_s in our experiment occurs on a much wider temperature range with respect to what assumed in [33], and to what observed in single crystals [22, 23]. Furthermore, R_s varies only by about 3 orders of magnitude from room temperature to 77 K. An estimation of ρ for the V_2O_3 layer performed using the measured R_s and thickness of the MIT layers of samples A and B leads to values that are of the order of 10^{-3} Ωm at room temperature. This is ~ 2 orders of magnitude higher than what reported in [19] for the V_2O_3 slurry and to what measured in single crystals [22, 23]. The large difference between the result of this work and what reported for V_2O_3 single crystals is not surprising, as the metal-to-insulator transition in V_2O_3 depends on many parameters, as the purity and the strain state [23, 24, 25, 26]. For example, very broad transitions, which take place down to ~ 10 K, were reported for the electrical resistivity of different V_2O_3 films prepared by reactive sputtering [24, 34].

In the light of the large variability of the electrical properties of V_2O_3, we believe that our results can contribute to assess, also through simulation codes, the electrical and thermal performance expected for REBCO pancake coils co-wound with a V_2O_3 inter-layer.

V. Conclusion

With the aim of providing magnet designers with information fundamental to evaluate the stability and performance of HTS magnets prepared using MIT materials, we investigated the contact resistance in sandwiches composed by two REBCO CCs and a V_2O_3 inter-layer. This configuration schematizes the one realized in a REBCO pancake coil. We proved that ~ 10 μm thick MIT layers can be easily deposited on commercial Cu-stabilized CCs by dip coating in colloidal solutions prepared with V_2O_3 powders with a granulometry in the 1 μm range. The technique employed in this work is potentially scalable (e.g., by spray coating) to long-conductor productions. R_s is mainly determined by the contribution of the MIT layer and varies by ~ 8 orders of magnitude when changing the temperature from ~ 10 K to ~ 250 K. Assuming that $R_s = 10^5$ μΩ·cm² defines the quench propagation limit, we find that an effective quench

propagation may be possible for hot-spot temperatures between 135 K and 175 K. A MIT layer whose thickness is in the 1 μm range should allow an effective quench propagation at temperatures close to the T_c of REBCO. Our attempt to enhance the viscosity of the colloidal solution by using the PVB polymer lead to a R_s too high to enable magnet self-protection. We believe that the information provided in this manuscript can help magnet designers to clarify the role that MIT materials may have in future HTS magnets. Indeed, tuning R_s with the temperature can be a chance to achieve self-protection in case of quenches, limiting the drawbacks inherent with the NI technique, as the unbalanced forces produced during a quench, the charge delay and the non-linear current-field dependence.

ACKNOWLEDGMENT

The authors warmly thank Damien Zurmuehle for technical assistance.

REFERENCES

[1] W Denis Markiewicz, Thomas Painter, Iain Dixon and Mark Bird, "Quench transient current and quench propagation limit in pancake wound REBCO coils as a function of contact resistance, critical current, and coil size," *Superconductor Science and Technology,* vol. 32, p. 105010, 2019.

[2] Yukikazu Iwasa, Case Studies in Superconducting Magnets, Cambridge, MA: Springer, 2009.

[3] M. Bonura and C. Senatore, "An equation for the quench propagation velocity valid for high field magnet use of REBCO coated conductors," *Applied Physics Letters,* vol. 108, p. 242602, 2016.

[4] S. Hahn, D. K. Park, J. Bascuñán, and Y. Iwasa, "HTS pancake coils without turn-to-turn insulation," *IEEE Trans. Appl. Supercond.,* vol. 21, p. 1592–1595, 2011.

[5] S. Yoon, J. Kim, H. Lee, S. Hahn and S-H Moon, "26 T 35 mm all-GdBa2Cu3O7–x multi-width no-insulation superconducting magnet," *Superconductor Science and Technology,* vol. 29, p. 04LT04, 2016.

[6] Seungyong Hahn, et al., "45.5-tesla direct-current magnetic field generated with a high-temperature superconducting magnet," *Nature,* vol. 570, p. 496, 2019.

[7] Seungyong Hahn,Kwangmin Kim, Kwanglok Kim, Haigun Lee, Yukikazu Iwasa, "Current Status of and Challenges for No-Insulation HTS Winding Technique," *Teion Kogaku,* vol. 53, no. 1, 2018.

[8] Xudong Wang, Seungyong Hahn, Youngjae Kim, Juan Bascuñán, John Voccio, Haigun Lee and Yukikazu Iwasa, "Turn-to-turn contact characteristics for an equivalent circuit model of no-insulation ReBCO pancake coil," *Superconductor Science and Technology,* vol. 26, p. 035012, 2013.

[9] Seokho Kim, Seungyong Hahn, Kwangmin Kim and David Larbalestier, "Method for generating linear current-field characteristics and eliminating charging delay in no-insulation superconducting magnets," *Superconductror Science and Technology,* vol. 30, p. 035020, 2017.

[10] W Denis Markiewicz, Jan J Jaroszynski, Dymtro V Abraimov, Rachel E Joyner and Amanatullah Khan, "Quench analysis of pancake wound REBCO coils with low resistance between turns," *Superconductor Science and Technology,* vol. 29, p. 025001, 2016.

[11] Thibault Lécrevisse, Xavier Chaud, Philippe Fazilleau, Clément Genot and Jung-Bin Song, "Metal-as-insulation HTS coils," *Superconductor Science and Technology,* vol. 35, p. 074004, 2022.

[12] Thomas Kurauchi and So Noguchi, "Unbalanced radial current flow simulation of no-insulation REBCO pancake coils during normal state transition," *Superconductor Science and Technology,* vol. 33, p. 104003, 2020.

[13] Marco Bonura , Christian Barth, A. Joudrier, Jose Ferradas Troitino , Alexandre Fete, and Carmine Senatore, "Systematic Study of the Contact Resistance Between REBCO Tapes: Pressure Dependence in the Case REBCO Tapes: Pressure Dependence in the Case and Metal-Insulation," *IEEE Trans. Appl. Supercond.,* vol. 29, no. 5, p. 6600305, 2019.

[14] Jun Lu, Robert Goddard, Ke Han and Seungyong Hahn, "Contact resistance between two REBCO tapes under load and load cycles," *Superconductor Science and Technology,* vol. 30, p. 045005 , 2017.

[15] Jun Lu, Jeremy Levitan, Dustin McRae and Robert Walsh, "Contact resistance between two REBCO tapes: the effects of cyclic loading and surface coating," *Superconductor Science and Technology,* vol. 31, p. 085006, 2018.

[16] Y. Suetomi, et al., "Quench and self-protecting behaviour of an intra-layer no-insulation (LNI) REBCO coil at 31.4," *Superconductor Science and Technology,* vol. 34, p. 064003, 2021.

[17] J.-B. Song et al., "Dynamic response of no-insulation and partial insulation coils for HTS wind power generator," *IEEE Trans. Appl. Supercond.,* vol. 25, no. 3, p. 5202905, 2015.

[18] Jae Young Jang, et al., "Design, construction and 13 K conduction-cooled operation of a 3 T 100 mm stainless steel cladding all-REBCO magnet," *Superconductor Science and Technology,* vol. 30, no. 10, p. 105012, 2017.

[19] Hyung-Wook Kim, Jin Hur, Seog-Whan Kim, Seok-Beom Kim, Rock-Kil Ko, Dong-Woo Ha, Ho Min Kim, Jin-Hong Joo, and Young-Sik Jo, "Improvement in Stability and Operating Characteristics of HTS Coil Using MIT Material," *IEEE Trans. Appl. Supercond.,* vol. 27, no. 4, p. 4601704, 2017.

[20] Hyung-Wook Kim, Young-Sik Jo, Seog-Whan Kim, Dong-Woo Ha, Rock-Kil Ko, Doohun Kim,and Jin Hur, "Enhancement of 2G HTS Coil Stability With V2O3 and Perforated HTS Wire," *IEEE Trans. Appl. Supercond.,* vol. 28, no. 3, p. 4600205, 2018.

[21] Hyung-Wook Kim , Young-Sik Jo , Seog-Whan Kim, Doohun Kim, and Jin Hur, "2G HTS Racetrack Coil Protection Using Smart Switching Feature of V2O3," *IEEE Trans. Appl. Supercond.,* vol. 29, no. 5, p. 4603305, 2019.

[22] S. Yonezawa, Y. Muraoka, Y. Ueda, and Z. Hiroi, "Epitaxial strain effects on the metal–insulator transition in V2O3 thin films," *Solid State Communications,* vol. 129, no. 4, pp. 245-248, 2004.

[23] B. S. Allimi, S. P. Alpay, C. K. Xie, B. O. Wells, J. I. Budnick, and D. M. Pease, "Resistivity of V2O3 thin films deposited on α-plane (110) and c-plane (001) sapphire by pulsed laser deposition," *Applied Physics Letters,* vol. 92, p. 202105, 2008.

[24] Jae-Hyun Haa, Hyung-Wook Kim, Young-Sik Jo, Seog-Whan Kim, Jung-Il Hong, "Tunable metal-insulator transition of V2O3 thin films strained by controlled inclusion of crystallographic defect," *Applied Materials Today,* vol. 22, p. 100984, 2021.

[25] S. Autier-Laurent, B. Mercey, D. Chippaux, P. Limelette, and Ch. Simon, "Strain-induced pressure effect in pulsed laser deposited thin films of the strongly correlated oxide V2O3," *Physical Review B,* vol. 74, p. 195109, 2006.

[26] J. Trastoy, Y. Kalcheim, J. del Valle, I. Valmianski, and Ivan K. Schuller, "Enhanced metal–insulator transition in V2O3 by thermal quenching after growth," *Journal of Materials Science,* vol. 53, p. 9131–9137, 2018.

[27] M. Bonura, P. Cayado, K. Konstantopoulou, M. Alessandrini, C. Senatore, "Heating-Induced Performance Degradation of REBa2Cu3O7−x Coated Conductors: An Oxygen Out-Diffusion Scenario with Two Activation Energies," *ACS Applied Electronic Materials,* vol. 4, pp. 1318-1326, 2022.

[28] D. Matera, M. Bonura, R. Černý, S. McKeownWalker, F. Buta, D. LeBoeuf, X. Chaud, E. Giannini, C. Senatore, "High-feld superconductivity in C-doped MgB2 bulk samples prepared by a rapid synthesis route," *Scientific Reports,* vol. 10, p. 17656, 2020.

[29] S. Xue; M. D. Sumption; D. Panik; C. J. Thong; X. Guo; M. Majoros; E. W. Collings, "Electrical Contact Resistance in REBCO Stacks and Cables With Modified Surfaces," *IEEE Trans. Appl. Supercond.,* vol. 32, no. 6, p. 4802506, 2022.

[30] Young-Sik Jo, et al., "Electrical Characteristics of Smart Insulation 2G HTS Coils Based on Three Fabrication Methods," *IEEE Trans. Appl. Supercon.,* vol. 29, no. 5, p. 4601505, 2019.

[31] Guruprasad Alva, Yaxue Lin, Guiyin Fang, "Thermal and electrical characterization of polymer/ceramic composites with polyvinyl butyral matrix," *Materials Chemistry and Physics,* vol. 205, pp. 401-415, 2018.

[32] Abesach Moshalagae Motlatle, Orebotse Joseph Bothloko, Manfred Rudolf Scriba, Vincent Ojijo, and Suprakas Sinha Ray, "The thermal degradation kinetics and morphology of poly(vinyl butyral) cast films prepared using different organic solvents," *AIP Conference Proceedings,* vol. 2289, p. 020071, 2020.

[33] Huu Luong Quach et al., "Electrical and thermal analyses of a second generation high temperature superconducting magnet with vanadium III oxide and Kapton polyimide film insulation materials under an over-pulse current," *Superconductor Science and Technology,* vol. 32, p. 065006, 2019.

[34] B. Sass, C. Tusche, W. Felsch, N. Quaas, A. Weismann and M. Wenderoth, "Structural and electronic properties of epitaxial V2O3 thin films," *J. Phys.: Condens. Matter,* vol. 16, pp. 77-87, 2004.